Holzforschung, Vol. 65, pp. 845–853, 2011 • Copyright © by Walter de Gruyter • Berlin • Boston. DOI 10.1515/HF.2011.104

Characterizing perpendicular-to-grain compression ($C_\perp$) behavior in wood construction

Craig Thomas Basta[1], Rakesh Gupta[1], Robert J. Leichti[2] and Arijit Sinha[1,*]

[1] Department of Wood Science and Engineering, Oregon State University, Corvallis, OR, USA
[2] StanleyBlack & Decker, East Greenwich, Rhode Island, USA

*Corresponding author.
Department of Wood Science and Engineering, Oregon State University, 119 Richardson Hall, Corvallis, Oregon 97331-5751, USA
Phone: +541-737-8423
Fax: +541-737-3385
E-mail: arijit.sinha@oregonstate.edu; arijitsinha@gmail.com

Abstract

Current compression perpendicular-to-grain ($C_\perp$) design values for wood members are based on mean stress obtained from ASTM D143 specimen. The standard ASTM test with metal on wood bearing has limited applicability in modern construction assemblies with $C_\perp$ loading scenarios. Previous work has shown that end-bearing conditions and wood-on-wood $C_\perp$ bearing is a more severe case as opposed to load applied over central area and metal-on-wood bearing. This study evaluated $C_\perp$ behavior of typical assemblies used in construction, in which members experience $C_\perp$ stresses near their longitudinal-end through wood-on-wood contact. These included assembly of the bottom chord of a truss bearing on the top plate of a wall (BC assembly) and assembly of the compression chord of a shear wall bearing on the bottom plate (BP assembly) of a wall. Three different BC assemblies were tested with varying aspect ratios (height/width) of the bottom chord (B.C.) member. For each test assembly, paired ASTM tests of the main member (bottom chord member in BC tests, and bottom plate member in BP tests) were conducted. The assembly stresses at 1 mm deflection were always lower than the corresponding ASTM stresses at the same deflection. Due to varying assembly depths, 1 mm deflection was a poor criterion for determining $C_\perp$ stress values. For B.C. members, when loaded tangentially, they buckle in the direction of annual ring curvature. High aspect ratios accentuate this effect. Expectedly, the tendency to buckle and the probability of total failure in the assembly increase with increasing aspect ratio. This behavior was not observed in the ASTM tests.

Keywords: construction applications; shear walls; wood-frame truss; wood-on-wood bearing.

Introduction

In contemporary wood-frame construction, compression perpendicular to grain ($C_\perp$) behavior plays an important role (Hoffmeyer et al. 2000; Leijten et al. 2010) and sometimes it governs design criteria (Fergus et al. 1981; Bulmanis et al. 1983; Blass and Gorlacher 2004). In the US design code for timber structures, National Design Specification (NDS), with the exception of $C_\perp$ and shear parallel to grain, current wood design values are based on full-scale specimen testing (AFPA 2005). Moreover, except for $C_\perp$ design values and modulus of elasticity in the NDS, all allowable stress values are derived based on 5% exclusion limit on property distribution curves (AFPA 2005). $C_\perp$ is based on testing of a $50\times50\times150$ mm ($2\times2\times6$ in) specimen using the ASTM D143 standard (ASTM 2010) where the load is applied in the middle through a steel plate of 50×50 mm in dimension. $C_\perp$ design value is based on stress at 1 mm (0.04 in) deflection ($\sigma_{0.04\text{-D}}$) as shown in Figure 1. At the time the ASTM standard (ASTM 2010) was developed, it reflected the practical applications of wood members subjected to $C_\perp$ loading, such as railroad cross-ties, wall plates and applications with aspect ratios (height/width) of one or less. Nowadays, however, the cross-sections in wood constructions (in which $C_\perp$ is effective) have aspect ratios much larger than one. Such applications include lumber as well as engineered wood products for floor joists, truss applications, I-joists, rim joists, etc.

A main drawback of the ASTM test specimen is that the metal-on-wood compression produced in this test inaccurately reflects the typical wood-on-wood compression often present in structural application (Fergus et al. 1981). The ASTM test was primarily designed to simulate the behavior of a wood joist resting on a masonry wall or concrete foundation (Bodig 1969) and does not intend to determine a physically correct perpendicular-to-grain strength (Leijten et al. 2010). In typical applications, it is mostly wood-on-wood contact such as in the bottom chord of a truss resting on the top plate of a shear wall. In trusses, span length is often limited by bearing stress at the interface of the bottom truss chord and the top plate of the supporting wall (Fergus et al. 1981). Design limitations due to transverse compression have provided impetus for design of connections aimed at increasing transverse compression strength (Bulmanis et al. 1983). When shear walls are subjected to shear forces, the end-posts serve alternatively as vertical tension and compression chords. For the latter, adequate bearing capacity of the chord on the top and bottom plates of the wall must be provided (Rose 1998). Tests conducted by APA demonstrated that for heavily loaded shear walls with sheathing on both sides, $C_\perp$ produced by the bearing of a compression chord against wall plates can be a design limiting concern (Rose and Keith 1996; Tissell 1996; Rose 1998; Breyer et al. 2003). These scenarios call for wood-on-wood bearing stress that is not directly measured by the ASTM method.

Brought to you by | Oregon State University
Authenticated | 128.193.162.72
Download Date | 11/8/12 6:03 PM

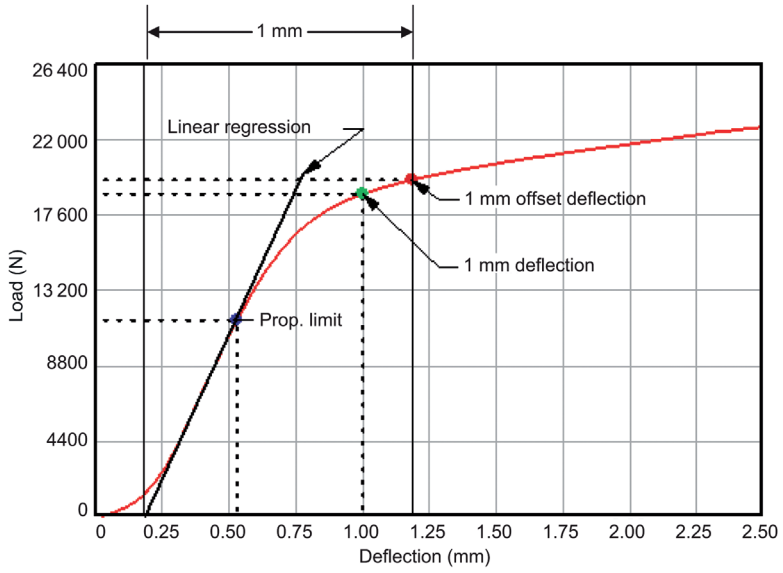

Figure 1 Typical load-deflection diagram for ASTM specimen depicting offset deflection stress determination.

Another peculiarity of the ASTM test is that the metallic loading block does not cover the entire area of the specimen; as a result, shear stresses as well as compressive stresses are developed. Shear stresses, which develop at the edges of the bearing plate, lead to higher $C_\perp$ values than in cases in which load is applied over the full area of the specimen (Kunesh 1968; Bodig 1969; Pellicane et al. 1994). In contrast, the CEN EN408 (CEN 2010) prescribes a method for $C_\perp$ where a block of timber is loaded in uniform compression over the full surface (Gehri 1997). However, in EN 408, the $C_\perp$ value is based on stress at deflection equivalent to 1% of the height of the sample. Blass and Gorlacher (2004) derived a mechanical model for partial surface loading $C_\perp$ scenarios and suggested a design approach based on the characteristic $C_\perp$ value of a full surface compression as per the European Standards. The ASTM D143 test has limited applicability to full surface compression as well as end-bearing compression scenarios. The NDS provides increases in allowable $C_\perp$ with bearing area factors (C_b) (AFPA 2005). However, there is no reduction factor provided for the case of $C_\perp$ bearing near the longitudinal-end of members.

There is a pressing need to characterize the $C_\perp$ value for real application scenarios involving wood-on-wood compression. This study specifically characterizes the behavior of structural lumber subjected to wood-on-wood compression. The objectives of this study are to evaluate $C_\perp$ behavior in the bottom chord of a truss bearing on the top sill plate of a wall and the compression chord of a shear wall bearing against the bottom plate of the wall by: (1) characterizing failure behavior; and (2) comparing $C_\perp$ strength of tested assemblies to corresponding ASTM tests and literature data.

Materials and methods

Two assemblies were evaluated that are very common in $C_\perp$ construction. Additionally, ASTM specimens were tested, which were prepared from the constituting materials of the two assemblies. The number of samples tested is listed in Table 1. Samples were cut in a fashion deemed consistent with construction practice with a table saw. The specimens were conditioned at 20°C and 65% relative humidity until daily weight became stable. Member dimensions (length, width, and thickness) were measured. The BC and BP

Table 1 Test matrices for bottom chord of truss on top plate of wall (BC assembly) and compression chord of truss on bottom plate of wall (BP assembly).

Douglas fir elements in assemblies			Number of samples (n)		Loading rate (mm min^{-1})[a]	
Dimension (mm)	Dimension (mm)	Symbol[b]	Assembly	ASTM[c]	Initial	Post
B.C. truss 38×89	T.P. wall 38×89	BC-2×4	20	20	3.3	33
B.C. truss 38×184	T.P. wall 38×89	BC-2×8	17	20	5.0	26
B.C. truss 38×292	T.P. wall 38×89	BC-2×12	20	20	7.5	7.2
B.P. 38×39	C.C. wall 38×89	BP-2×2	20	20	0.76	7.6

[a]After 10% compression strain has been reached.
[b]Dimensions from mm converted into inches and rounded up to a whole number.
[c]Prepared from B.C. or B.P. members, respectively.
T.P., top plate; B.C., bottom chord; B.P., bottom plate; C.C., compression chord.

Brought to you by | Oregon State University
Authenticated | 128.193.162.72
Download Date | 11/8/12 6:03 PM

assemblies, made of Douglas fir (*Pseudotsuga menziesii*), were tested.

BC assembly

The bottom chord of truss on top plate of wall (BC assembly) is shown in Figure 2a. The member representative of the bottom chord in this design is hereafter referred to as ''B.C. member'' while those of the top plate will be referred to as ''T.P. member''. The longitudinal-end of the B.C. member is sandwiched between the T.P. members. Load was applied through a metal plate to the full surface on one wide face and wood-on-wood partial surface compression on the other wide face of the T.P. member (Figure 2a). This condition is similar to the ASTM test specimen. Both narrow faces of the longitudinal-end of the B.C. member are loaded (Figure 2a); this is not possible in the case of the ASTM specimen. Bearing is through wood-to-wood contact as opposed to metal-on-wood for the ASTM specimen. Three different B.C. members were tested (see Table 1). Aspect ratios of B.C. members vary (2.3, 4.8 and 7.5) for the member dimensions (given as rounded digits in inches) 2×4, 2×8 and 2×12, respectively, as opposed to an aspect ratio of one for the ASTM specimen.

BP assembly

The conditions of the ''compression chord of truss on bottom plate of wall'' (BP assembly) are shown in Figure 2b. A member with dimensions of 75×38×89 mm^3 (in rounded digits of inches: 3×2×4), representative of the longitudinally loaded compression chord (C.C.) of a shear wall, rests on the wide face of the bottom plate (B.P.) with dimensions 150×38×89 mm^3 (6×2×4 in inches). The C.C. member bears at the longitudinal-end of the B.P. member. The B.P. member's lower surface was fully supported by a rigid metal plate. The longitudinal-end of the B.P. member away from the C.C. member bearing was clamped to prevent uplift. This represents the effect of anchor bolts, which clamp the bottom sill plate to the foundation. Load was applied through a metal plate to the top surface of the C.C. member. Load was applied through the longitudinally loaded C.C. member to the top surface of the B.P. member through wood-to-wood bearing as opposed to metal-on-wood

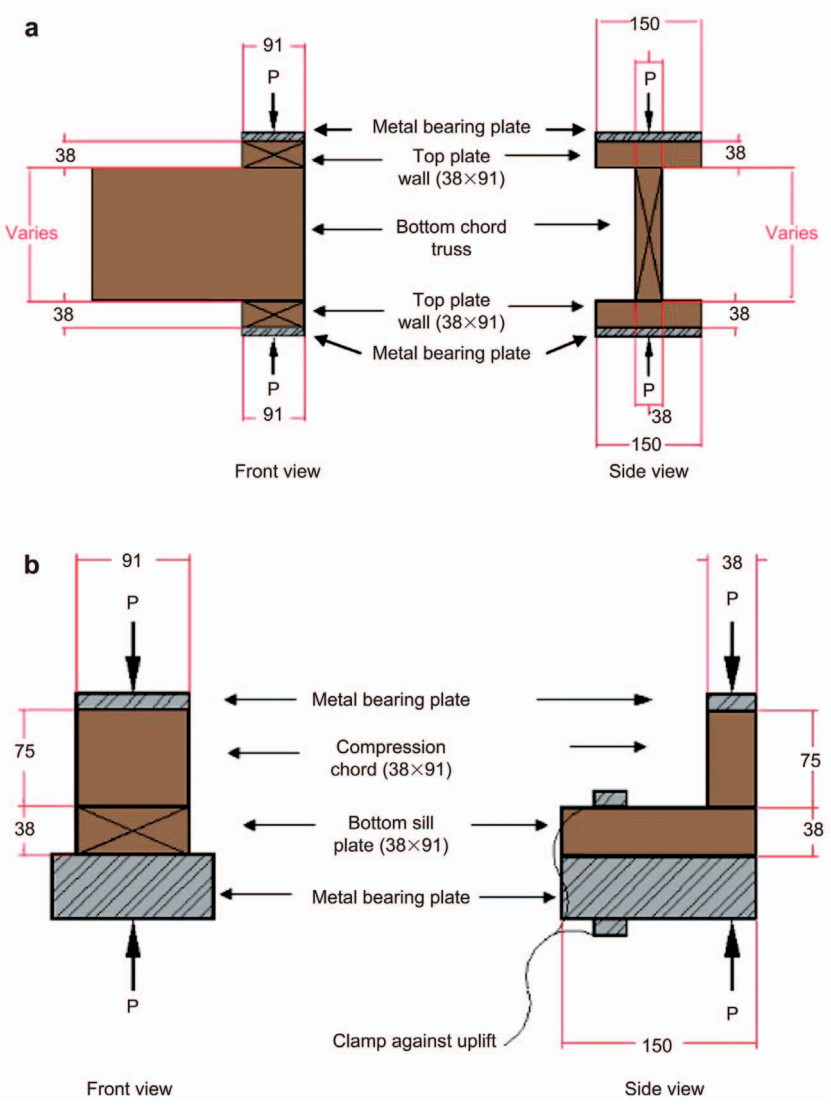

Figure 2 Schematics of the assemblies tested (a) BC assembly, truss bottom chord on wall top plate and (b) BP assembly, compression chord bearing on bottom plate of wall.

Brought to you by | Oregon State University
Authenticated | 128.193.162.72
Download Date | 11/8/12 6:03 PM

bearing for the ASTM specimen. Both wide faces of the longitudinal-end of the B.P. member are stressed, as shown in Figure 2b. This condition is not fulfilled by the ASTM specimen. The sill plate was fastened to the bottom surface to prevent vertical movement and rotation. Also here, a corresponding ASTM test was conducted on a sample cut from the same board as the B.P. member.

Test set-up

The load was applied by an MTS (Eden Prairie, Minnesota, USA) hydraulic actuator (Figure 3a,b). For BC assemblies, the lower top plate member rests on a metal base plate and is held in position by movable magnetic stops. To minimize the initial misalignment, the test head was brought flush with the upper top plate member and the truss bottom chord and upper-top-plate positioned. The test head could translate only vertically but it could not rotate. Figure 3c shows the BP assembly test set-up. The bottom plate member rests on a metal base plate with movable magnetic stops holding the compression chord and bottom plate member in their respective positions. The compression chord could only translate vertically.

The compressive load and total assembly deflection was measured. Data were routed through a Schaevitz LVDT signal conditioner (Hampton, Virginia, USA) to a National Instruments AT-MIO/AI 16-50E computer (Austin, Texas, USA). The loading deflection rates are listed in Table 1. The initial and post loading compressive strain were each 10%. The testing was continued until the assembly failed. ASTM specimens were tested according to ASTM D143 but with depth of the sample of 38 mm due to availability of standard dimensional lumber and a constant cross-head displacement rate of 7.6 mm min^{-1}. Load and compressive deflections were recorded throughout testing. Testing was documented with digital photos and videos. The linear range in the stress-strain diagram was identified by visual inspection. Stress offsets were defined by means of a linear regression for data fitting. The offset load is defined as the intersection of load-deformation curve (P-Δ) and a line parallel to the initial linear portion of the P-Δ curve offset by a certain value in the positive direction. For all tests, load at 1 mm (0.04 in) deflection ($P_{0.04\text{-}D}$) and load at 1 mm system-offset-deflection ($P_{0.04\text{-}OD}$) were recorded. The stress corresponding to both these deflections, a system-deflection ($\sigma_{0.04\text{-}D}$) and an offset-deflection ($\sigma_{0.04\text{-}OD}$), was calculated by dividing load by area of loading. All total failures with corresponding system strains and stresses were recorded.

Results and discussion

Compression behavior of BC assemblies

Top plate (T.P.) Compression behavior was similar for all T.P. members throughout BC tests. They exhibited densification in the loaded area similar to that in a standard ASTM test (Figure 4). The densification in T.P. members was uneven with higher densification away from loaded longitudinal-end of the B.C. member (Figure 4). This behavior was interpreted based on finite element analysis of Basta (2005), that B.C. members resisted more compression farther from the loaded longitudinal-end. Shearing forces in the B.C. wood fiber along the edge of the compression zone away from the B.C. longitudinal-end help support and stiffen the compressive resistance of this end. Relative deformation in two contacting compressed members (T.P. and B.C. members) was determined by the relative stiffness of the two contacting materials, and the T.P. members showed greater compressive deformation farther from the loaded longitudinal-end of the B.C. member. In some cases, when B.C. members were loaded near tangentially, earlywood (EW) and

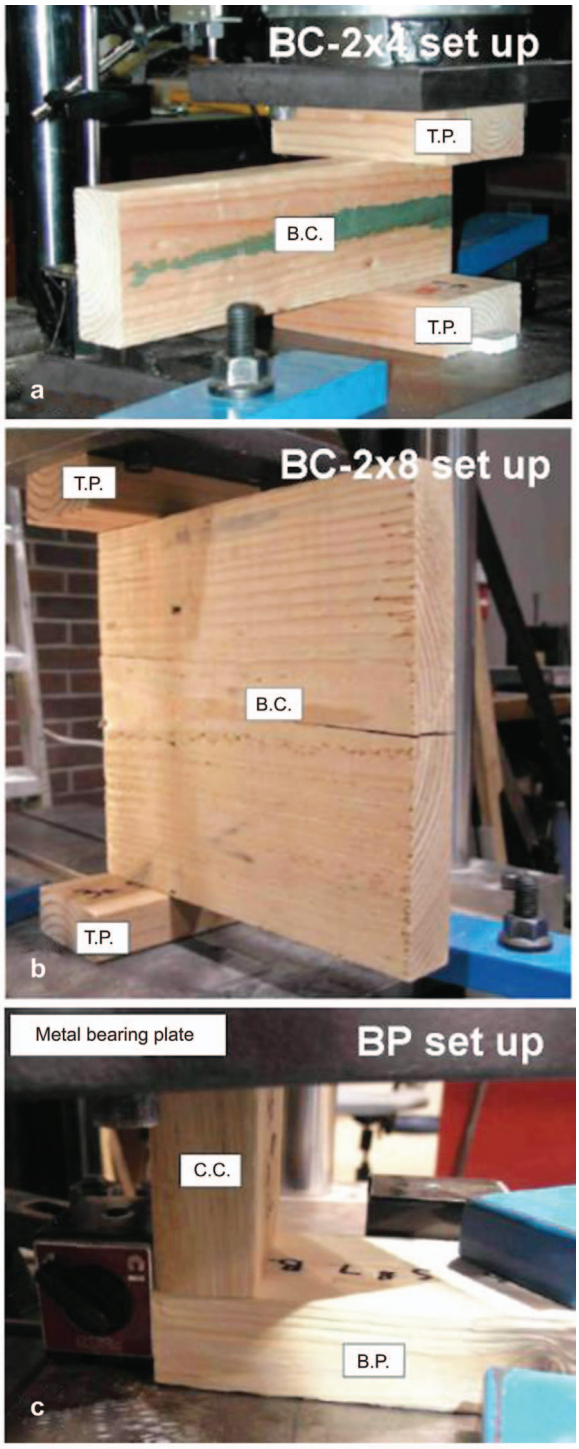

Figure 3 Photographic illustration of the experimental set ups shown in Figure 1. (a) and (b) BC set ups, where BC means 'bottom chord of truss on top plate of wall' and 2×4 resp. 2×8 refers to the sample dimension in inches (rounded digits); B.C., bottom chord member; T.P., top plate. (c) BS set-up, where BS means 'compression chord of truss on bottom plate of wall'.

Brought to you by | Oregon State University
Authenticated | 128.193.162.72
Download Date | 11/8/12 6:03 PM

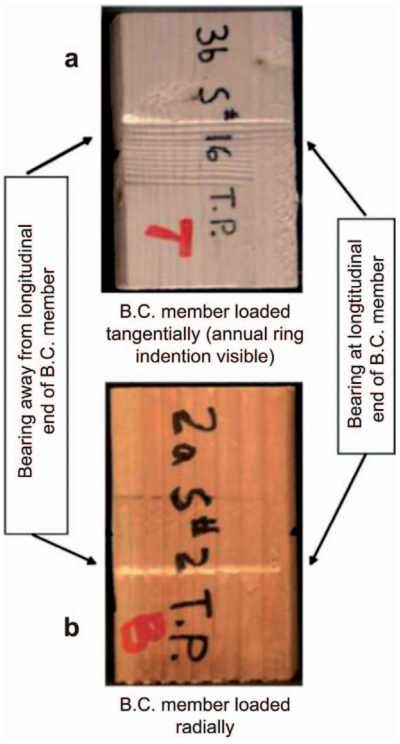

Figure 4 Top plate (T.P.) behavior in BC assembly. (a) B.C. member loaded tangentially; (b) B.C. member loaded radially.

latewood (LW) indentations could often be distinguished in the T.P. members. This is because the LW layers in B.C. members act as reinforcing columns within the gross wood material in tangential loading (Bodig 1965; Kennedy 1968; Tabarsa and Chui 2001) and leave deeper indentation when in contact with T.P. members.

Bottom chord (B.C.) members Observed compression behavior of B.C. members varied depending upon ring orientation. The failure behavior of 2×8 assembly was similar to 2×4 and sometimes 2×12 assemblies, as will be discussed later. Failure patterns are presented in Figures 5 and 6 (for member dimensions of 2×4 and 2×12, respectively). A detailed illustration of 2×8 assembly failure is provided by Basta (2005). When loaded tangentially, damage to B.C. members was seen as buckling of annual rings with corresponding shear along the EW-LW interface (Figure 5a,e and Figure 6b,f) due to LW layers acting as reinforcing columns in this orientation that tended to buckle under higher stresses (Bodig 1965; Kennedy 1968; Tabarsa and Chui 2001). Annual rings buckled in the direction of their pre-existing curvature with higher ring curvature leading to more severe buckling. Buckling was more severe on the surface, where the ring orientation deviated farthest from the plane (Figure 5f). Similar to 2×4 assemblies, when B.C. members 2×8 and 2×12 tests were loaded nearly parallel to ring orientation, damage was seen as buckling of annual rings with corresponding rolling shear along the EW-LW interface (Figure 6c). In 2×12 members localized buckling of annual rings was seen at areas of highest annual ring angle to loading plane (Figure 6b,f). This led to rolling shear and cross-grain bending of the B.C. member (Figure 7a,b,f).

B.C. members loaded at higher angles to ring orientation exhibited crushing of annual rings with corresponding densification (Figure 5b,c). Such specimens had a tendency to crack through the pith when pith was present due to the Poisson effect, leading to tensile stresses in the direction orthogonal to applied load. B.C. members also had a tendency to split at the unloaded end of the member with the split propagating longitudinally along the minor axis but stopping short of the loaded end (Figure 5d). This behavior is due to transverse tension stresses in the direction of applied load arising from continued densification of the loaded longitudinal-end of the member. A simultaneous drop in load, which was quickly recovered and often exceeded the splitting load as testing continued, accompanied the splitting in all the three test assemblies. Around 30% of 2×4 and about 70% of 2×8 and 85% of 2×12 members split longitudinally in this manner. This splitting did not lead to immediate total failure in 2×8 members, although it may have contributed to the global failure. The tendency of B.C. members to split longitudinally along the major axis was accentuated by high aspect ratios of B.C. members 2×12 (Figure 6d), with one or more longitudinal splits often developing along the major axis of 2×12 members. This splitting effect observed in all BC assemblies may not occur in longer pieces used in construction practice.

BC-2×4 assemblies had a relatively low aspect ratio of 2.3 in the B.C. member and exhibited continual densification without total failure. Stress carrying capacity often increased, at least initially, with increasing system densification. Well beyond the linear region in the load-deflection diagram (Figure 8), assembly stress increased and decreased as annual rings buckled and/or sheared along the EW-LW interface. No total failures were observed in BC-2×4 assemblies. However, with the increased aspect ratio to 4.8 and 7.5 (2×8 and 2×12 members, respectively) the annual ring buckling effects were pronounced. In 2×8 and 2×4 assemblies, the B.C. members did not fail totally, except in three tests. In one of the assemblies, annual ring buckling led to total rolling shear failure of the B.C. member at a system strain of 7.7% with maximum stress being attained at 5.1% system strain. The higher aspect ratio for 2×12 members led to cross-grain bending of B.C. members with corresponding rolling shear and a high percentage (90%) of total failure for all ring orientations, especially for 2×12 members. In 18 of the 20 tests, total failures were observed prior to reaching 10% system strain while in the other two, the 2×12 assembly supported load to 10% system strain. Additionally, three 2×12 members failed totally before reaching the design value for compression perpendicular of 4137 kPa (600 psi, AFPA 2005).

Compression behavior of BP assembly

The observed compression mode in BP members (Figure 7) was that of continuous densification with increasing load and eventual shear of the B.P. occurred along the front edge of the C.C. (Figure 7a,b,d,f) without total failure. This general mode of compression was observed for all B.P. members.

Brought to you by | Oregon State University
Authenticated | 128.193.162.72
Download Date | 11/8/12 6:03 PM

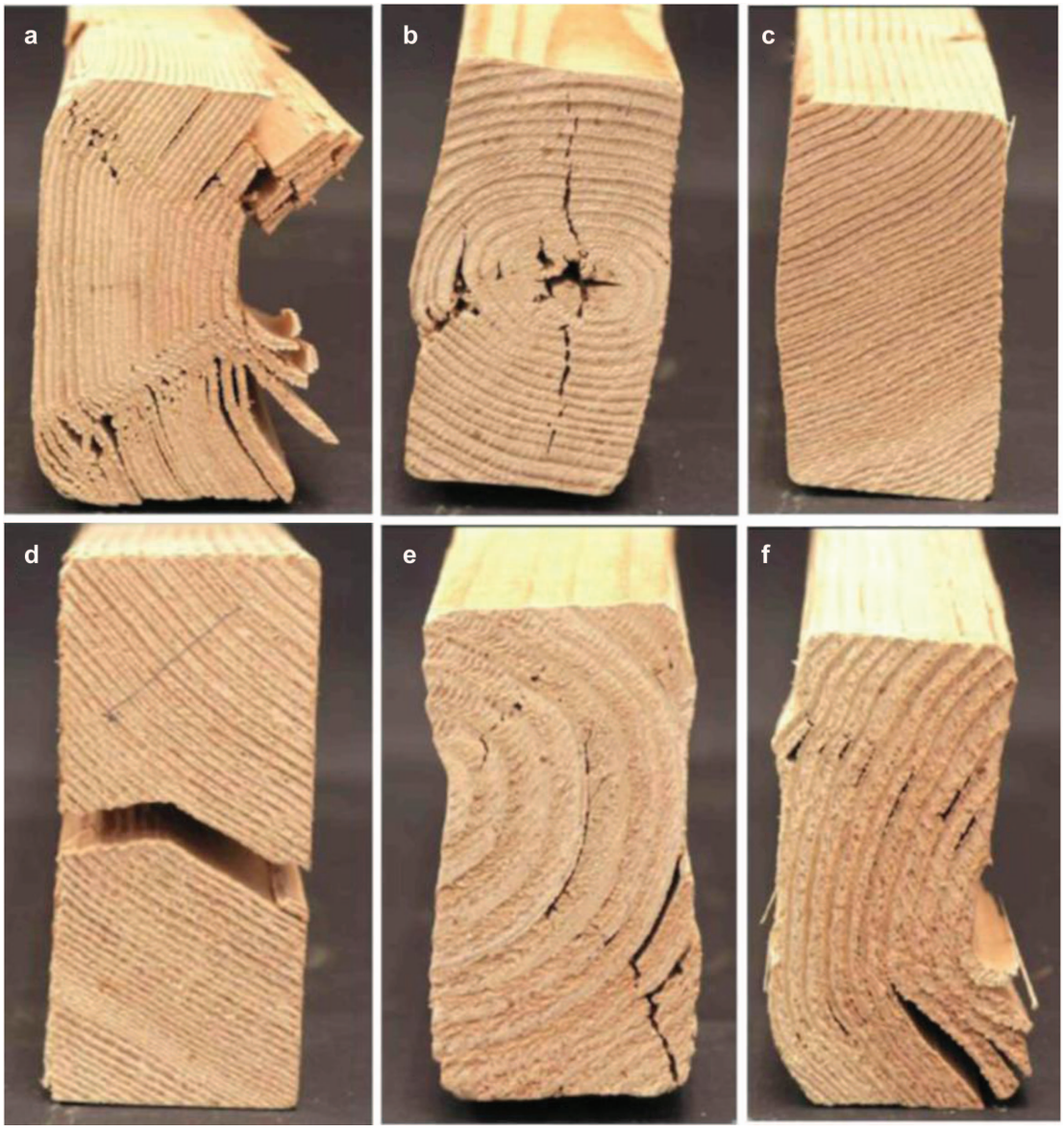

Figure 5 Characteristic compression damage in BC-2×4 assembly B.C. members. (a) Annual ring buckling and shear; (b) tension crack through pith; (c) densification; (d) tension perp. splitting; (e) rolling shear and tension perp. cracking; (f) annual ring buckling and shear at bottom loaded face.

Splitting of B.P. members longitudinally along their major axis at higher strains (Figure 8c,e) was also observed. This behavior is attributed to the Poisson effect and/or cross-grain bending (resulting from pre-existing cupping in members) which led to tension perpendicular to grain failure. In three 2×2 assemblies, longitudinal splitting of the B.P. member led to longitudinal splitting of the C.C. (Figure 7e). The compression behavior of B.P. is similar to that observed for typical ASTM specimens. The B.P. members supported increasing stress even after they split longitudinally. In construction systems, longitudinal splitting of the B.P. could lead to system failure under shear loads because anchor bolts lose bearing capacity. Although B.P. specimens were only 150 mm long, even the longer members have shown this longitudinal splitting behavior (Redler 2011). Assembly stress invariably increased with increasing B.P. densification well beyond the linear region in the stress-strain diagram. There was a general trend of increasing assembly stress up to a system strain of 25% and this led to deliberate test termination. No total failures were seen in B.P. assemblies. Bottom plate assemblies exhibited large deflections prior to near linearity in the stress-strain diagram. These assemblies invariably deflected much more than ASTM specimens for a given stress. For given stresses, deflections in BP assemblies were often two or more times larger than that seen in corresponding ASTM tests.

Comparison with ASTM test specimens

Load-deflection diagrams (Figure 8) for ASTM and $C_{\perp}$ assemblies tested, illustrate the extreme differences between

Brought to you by | Oregon State University
Authenticated | 128.193.162.72
Download Date | 11/8/12 6:03 PM

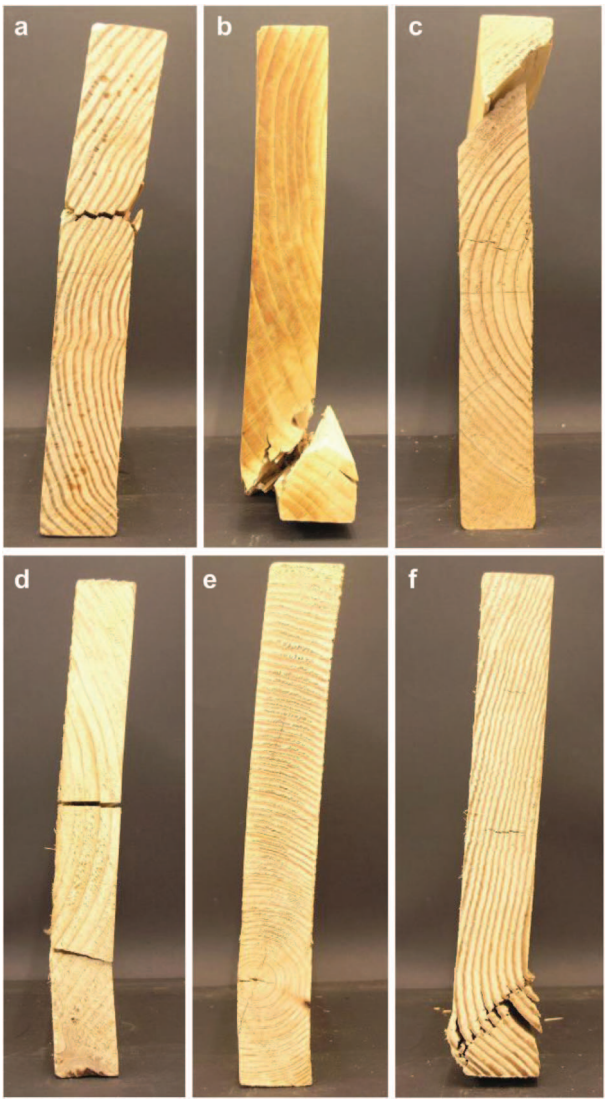

Figure 6 Characteristic compression damage in BC-2×12 assembly B.C. members. (a) Buckling of annual rings leading to tension-perp./rolling shear failure; (b) localized buckling of annual rings at highest ring angle leading to rolling shear failure; (c) rolling shear failure along earlywood/latewood interface at ring angle near 45 degrees; (d) tension perp. splitting throughout long length; (e) rolling shear; (f) local annual ring buckling and shear at bottom loaded face.

the behaviors of ASTM tests and BC and BP assemblies. Load at 1 mm (0.04 in) deflection for ASTM test and BC and BP assemblies are very different. Comparing the load at 1 mm deflection for ASTM specimen and BC-2×12, for instance, are approximately 19 000 N and 1700 N, respectively. On the other hand, the BP assembly attains a load around 2600 N at the same deflection. The ASTM values are similar to those published by Lum (1995), while the assembly values are a bit lower than that predicted by Lum and Karacabeyli (1994). Previously, interest has developed in basing allowable stress in compression perpendicular to grain on acceptable deformation for particular situations (Bendtsen and Haskell 1978; Bendtsen and Galligan 1979) rather than 1 mm deflection. The explanation for this extreme difference in $P_{0.04\text{-}D}$ is two-fold. First, compressibility of the members is highly dependent on member depth. With increasing member depth and multiple members in the connection, depth of the assembly increases. The total depth of BC-2×12 assemblies is 362 mm compared with 38 mm deep ASTM tests. The second reason for the difference is related to the initial range of non-linearity and upward curvature in the load-deflection diagrams (Figure 8). The multiple wood member assemblies examined in this study lead to larger misalignment and settling effects than the standard ASTM metal-on-wood tests. As a result, larger ranges of non-linearity prior to linear region of the load-deflection diagrams were observed. This phenomenon was highlighted in BP assemblies, because the BP specimens were cut in a manner consistent with construction practice, i.e., cut with a table saw, rough and non-rectilinear surfaces were present at the contact surface between the C.C. and B.P. members. Large settling effects in BP tests led to unusually larger regions of initial alignment, which pushed the near linear range out farther on the load axis. To adjust for settlement effects in all assemblies, a comparison of testing configurations and assemblies seemed to be adequate based on offset displacements. This measure is defined as the difference in displacement between the origin and intersection of regression line with displacement axis.

The stress value at 1 mm offset deflection is obtained by dividing the load (at offset) by the nominal area of loading for the member and is presented in Table 2 along with their coefficient of variations (COV). The COV is lower for the $\sigma_{0.04\text{-}OD}$ as compared to the $\sigma_{0.04D}$ for all test assemblies. This is because the misalignment region results in large variability. After accounting for the initial misalignments by calculating offset deflection stress, a reduced variability is observed. COV of ASTM 2×8 and 2×12 tests exceeded the reported value of 28% (Green et al. 1999) for $\sigma_{0.04\text{-}D}$ and $\sigma_{0.04\text{-}OD}$. This resulted from the variable ring angle of ASTM tests conducted in this study whereas the ASTM testing procedure specifies load applied only parallel to the annual rings.

The $C_\perp$ behavior of structural lumber in practical applications is vastly different from that of the ASTM test specimen. The members, especially B.C. members, tend to buckle with the growth rings and fails in rolling shear. As the aspect ratio increased in BC assemblies, the mean stress decreased and the occurrence of total failure increased, whereas the ASTM specimen seldom fails totally. In contrast, densification of wood on contact to metal loading block leads to an increase in stress carrying capacity of the ASTM specimen. As the depth of the assembly, especially in B.C. members, increased, the stresses encountered at a given deflection decreased. However, the tendency of BC-2×12 members to buckle overshadowed the effect of the increased depth in the members. When cross-grain bending occurs, this mode of compressive deflection dominates compressive behavior. Compressive deflection occurs predominantly through further cross-grain bending in the B.C. member, rather than compressive deflection throughout the depth of the members.

Brought to you by | Oregon State University
Authenticated | 128.193.162.72
Download Date | 11/8/12 6:03 PM

Figure 7 Behavior of BP assembly. (a) Typical densification with shear at front edge of C.C.; (b) typical densification with shear at front edge of C.C; (c) longitudinal splitting of B.P. along major axis; (d) typical densification with shear at front edge of C.C; (e) longitudinal splitting of B.P. leading to longitudinal splitting of C.C.; (f) typical indentation of C.C. into B.P.

Further study is needed to better understand the relationship between member depth and stress in $C_{\perp}$ loading.

Conclusions

The behavior of compression perpendicular to grain ($C_{\perp}$) was studied in practical construction assemblies. The assembly stresses at 1 mm (0.04 in) deflection were always lower than the corresponding ASTM stresses at the same deflection. Large settlement effects (initial misalignment region) were observed in the wood-on-wood test assemblies. An offset displacement successfully adjusts for these effects and lowers the variability. The behavior of T.P. members in BC assembly and B.P members in BP assembly was similar to that seen in the ASTM specimen. However, the compression was uneven with more densification on the side of the T.P. member away from the loaded end of the B.C. member. This behavior shows that the adjacent unloaded material in the B.C. member provides support to the volume directly under the T.P. bearing surface. B.P. members had a tendency to split longitudinally along their major axis due to transverse tensile forces that develop within the B.P. member as it densifies. The B.C. members, when loaded tangentially, buckle in the direction of annual ring curvature. High aspect ratios accen-

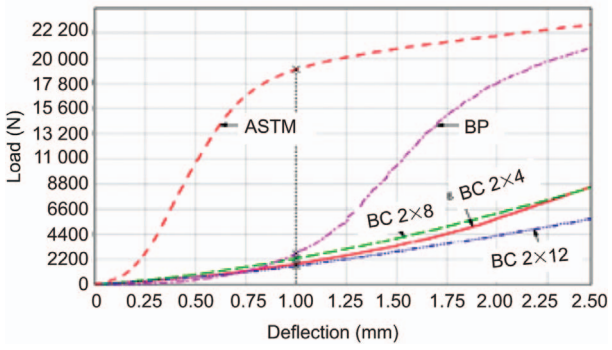

Figure 8 Load-deflection diagrams for all the assemblies tested.

Brought to you by | Oregon State University
Authenticated | 128.193.162.72
Download Date | 11/8/12 6:03 PM

Table 2 Stress value perpendicular to grain ($C_\perp$) at 1 mm deflection (0.04 in) and 1 mm offset-deflection and corresponding coefficients of variation (COV) for the assemblies BC and BP, and ASTM samples, which had a loading area of 50× 50 mm.

		$C_\perp$ for assemblies				$C_\perp$ for ASTM			
Assembly and dimensions (in)	*n*	$\sigma_{0.04D}$ (kPa)	COV%	$\sigma_{0.04D\text{-}OD}$ (kPa)	COV%	$\sigma_{0.04D}$ (kPa)	COV%	$\sigma_{0.04D\text{-}OD}$ (kPa)	COV%
BC-2×4	20	862	45	1951	34	6647	22	7260	24
BC-2×8	17	531	35	1393	25	6357	35	7950	31
BC-2×12	20	421	46	993	32	5474	42	7226	35
BP-2×2	20	1034	34	5316	31	6647	22	7260	24

tuate this effect and the combination of ring curvature and aspect ratio had a tendency to produce rolling shear failure in B.C. members along the earlywood–latewood interface. Moreover, B.C. members had a tendency to split longitudinally along their major axis. This phenomenon did not lead to immediate total failure of B.C. members but it may have contributed to global failure. Unlike in ASTM tests, with the increase in aspect ratio, tendency to buckle increases as well as the probability for total failure in the assembly.

References

American Forest and Paper Association (AFPA) (2005) National design specification for wood construction. AFPA, Washington, DC.

American Society for Testing and Materials (ASTM) (2010) D 143 Standard methods of testing small clear specimens of timber. ASTM, West Conshohocken, PA, USA.

Basta, C.T. (2005) Characterizing perpendicular to grain compression in wood construction. MS Thesis, Oregon State University, Corvallis, OR.

Bendtsen, B.A., Galligan, W.L. (1979) Modeling of the stress-compression relationship in wood in compression perpendicular to grain. Forest Prod. J. 29:42–48.

Bendtsen, B.A., Haskell, J.H. (1978) Characterizing the stress-compression relationship of wood in compression perpendicular to grain. Wood Sci. 10:111–121.

Blass, H.J., Gorlacher, I.R. (2004) Compression perpendicular to the grain. Proceedings of the 8th World Conference of Timber Engineering 2:435–440.

Bodig, J. (1965) Initial stress-strain relationship in transverse compression. Forest Prod. J. 15:197–202.

Bodig, J. (1969) Improved load-carrying capacity of wood in transverse compression. Forest Prod. J. 19:39–44.

Breyer, D.E., Fridley, K.J., Pollock, D.G., Cobeen, K.E. (2003) Design of wood structures. The McGraw-Hill Companies, San Fransisco, CA, USA.

Bulmanis, N.S., Latos, H.A., Keenan, F.J. (1983) Improving the bearing strength of supports of light wood trusses. Can. J. Civ. Eng. 10:306–312.

Comité Européen de Normalisation (CEN) (2010) EN 408: timber structures – Structural timber and glued laminated timber – Determination of some physical and mechanical properties. CEN, Brussels.

Fergus, D.A., Senft, J.F., Suddarth, S.K. (1981) Recommended bearing stresses for design in light-frame construction. Forest Prod. J. 31:50–57.

Gehri, E. (1997) Timber in compression perpendicular to grain. In: Proceedings of International Conference of IUFRO S5.02 Timber Engineering, Copenhagen, Denmark, June 18–20. pp. 355–374.

Green, D.W., Winandy, J.E., Kretschmann, D.E. (1999) Mechanical properties of wood – wood as an engineering material. General Technical Report FPL-TR 113, US Department of Agriculture, Forest Service. Forest Products Laboratory, Madison, WI.

Hoffmeyer, P., Damkilde, L., Pedersen, T.N. (2000) Structural timber and glulam in compression perpendicular to grain. Holz Roh-Werk. 58:73–80.

Kennedy, R.W. (1968). Wood in transverse compression – Influence of some anatomical variables and density on behavior. Forest Prod. J. 18:36–40.

Kunesh, R.H. (1968) Strength and elastic properties of wood in transverse compression. Forest Prod. J. 18:65–72.

Leijten, A.J.M., Larsen, H.J., Van der Put, T.A.C.M. (2010) Structural design for compression strength perpendicular to the grain of timber beams. Constr. Build. Mater. 24:252–257.

Lum, C. (1995) Compression Perpendicular-to-Grain Design in CSA-086.1-M94. Forintek Canada Corp, Vancouver, BC.

Lum, C., Karacabeyli, E. (1994) Development of the ''critical bearing'' design clause in CSA-086.1. In: CIB Working Commission (W18A) – Timber Structures in Sydney, Australia. Forintek Canada Corp, Vancouver, BC.

Pellicane, P.J., Bodig, J., Mrema, A.L. (1994) Modeling wood in tranverse compression. J. Testing Eval. 22:376–382.

Redler, H. (2011) Cyclic tests of engineered shear walls with different bottom plate and anchor bolt washer sizes. MS Thesis, Oregon State University, Corvallis, OR.

Rose, J.D. (1998) Preliminary testing of wood structural panel shear walls under cyclic (reversed) loading. Laboratory Report 158. APA-The Engineered Wood Association, Engineered Wood Systems, Tacoma, WA.

Rose, J.D., Keith, E.D. (1996) Wood structural panel shear walls with gypsum wallboard and window/door openings. Laboratory Report 157. APA-The Engineered Wood Association, Tacoma, WA.

Tabarsa, T., Chui, Y.H. (2001) Characterizing microscopic behavior of wood under transverse compression. Part II. Effect of species and loading direction. Wood Fiber Sci. 33:223–232.

Tissell, J.R. (1996) Structural panel shear walls. Laboratory Report 154. APA-The Engineered Wood Association, Tacoma, WA.

Received November 9, 2010. Accepted April 26, 2011.
Previously published online July 19, 2011.

Brought to you by | Oregon State University
Authenticated | 128.193.162.72
Download Date | 11/8/12 6:03 PM